ISSN 0006-2979, Biochemistry (Moscow), 2024, Vol. 89, No. 5, pp. 923-932 © Pleiades Publishing, Ltd., 2024.

Quantitative Analysis of Phagocytosis in Whole Blood Using Double Staining and Visualization

Elena V. Lysakova[1], Alexander N. Shumeev[2], Sergei A. Chuvpilo[1], Viktor S. Laktyushkin[2], Natalia A. Arsentieva[3], Mikhail Yu. Bobrov[1], and Stanislav A. Rybtsov[2,a]*

[1]*Immunobiology and Biomedicine Division, Center for Genetics and Life Sciences, Sirius University of Science and Technology, 354340 Sirius, Krasnodar Region, Russia*

[2]*Resource Center for Cell Technologies and Immunology, Sirius University of Science and Technology, 354340 Sirius, Krasnodar Region, Russia*

[3]*Saint-Petersburg Pasteur Institute, 197101 St. Petersburg, Russia*

[a]*e-mail: rybtsov.sa@talantiuspeh.ru*

Received November 3, 2023
Revised January 9, 2024
Accepted February 19, 2024

Abstract—Phagocytosis is an essential innate immunity function in humans and animals. A decrease in the ability to phagocytize is associated with many diseases and aging of the immune system. Assessment of phagocytosis dynamics requires quantification of bacteria inside and outside the phagocyte. Although flow cytometry is the most common method for assessing phagocytosis, it does not include visualization and direct quantification of location of bacteria. Here, we used double-labeled *Escherichia coli* cells to evaluate phagocytosis by flow cytometry (cell sorting) and confocal microscopy, as well as employed image cytometry to provide high-throughput quantitative and spatial recognition of the double-labeled *E. coli* associated with the phagocytes. Retention of pathogens on the surface of myeloid and lymphoid cells without their internalization was suggested to be an auxiliary function of innate immunity in the fight against infections. The developed method of bacterial labeling significantly increased the accuracy of spatial and quantitative measurement of phagocytosis in whole blood and can be recommended as a tool for phagocytosis assessment by image cytometry.

DOI: 10.1134/S0006297924050122

Keywords: phagocytosis, *E. coli*, flow cytometry, confocal microscopy, human leukocytes

INTRODUCTION

Phagocytosis is common in animals and can be found in protozoans and multicellular organisms. Such mammalian phagocytic cells as (monocytes, macrophages, neutrophils, dendritic cells) are components of the innate immune system and the first line of defense against a variety of pathogens that enter the body and can cause dangerous infections. Phagocytosis is also required for elimination of apoptotic and senescent cells. Hence, phagocytosis is an indispensable process for maintaining homeostasis in multicellular animals [1]. A decrease in the ability of immune cells to phagocytize is associated various disorders, including organism's immunodeficient state in infectious diseases. Thus, reduced phagocytosis was found in the periodontal disease [2], lower airway bacterial colonization [3], and other conditions leading to serious pathologies [4, 5].

Foreign agents invading the body are recognized by "professional" phagocytes through a variety of Toll-like receptors (TLRs) located on the surface of the phagocyte. TLRs interact with bacterial cell wall components, e.g., lipopolysaccharide (LPS – while Fc receptors

Abbreviations: AF405, Alexa Fluor 405; DN, double-negative; Dim cells, cells whose fluorescence intensity is one order of magnitude brighter than the intensity of DN cells; DP, double-positive for FITC and AF405; PBS, phosphate buffered saline.

* To whom correspondence should be addressed.

recognize antibodies that opsonize pathogen's antigens [6]. Initiation of inflammation through the alternative mechanisms also primarily activates phagocytosis. Phagocytosis is an essential and basic mechanism that helps to eliminate a pathogen or to suppress its spread. Therefore, many infections have evolutionarily developed the pathways that provide phagocytosis suppression as the main protective mechanism against the host's immunity [7, 8]. Inhibition of phagocytosis is also one of the main mechanisms used by tumors to escape immune recognition and removal [9].

Phagocytosis is an important link between innate and adaptive immunity. Phagocytized pathogens are processed into short peptides that are displayed on the surface of phagocyte in the context of the histocompatibility complex class II (MHC II) and are presented to T lymphocytes, thus initiating T cell proliferation and triggering adaptive immune response [10]. Therefore, assessment of phagocytic activity is an extremely important diagnostic technique that can be used in preventing immune pathologies, studying the mechanisms of development of dangerous diseases, and testing drugs that modulate innate immunity and phagocytosis.

The phagocytic activity of leukocytes is usually assessed using special phagocytic tests [11, 12]. There are multiple variations of this assay that use different targets of phagocytosis. For example, *Escherichia coli* is commonly employed as a safe and effective target for phagocytosis in research tests. The cell wall of *E. coli* contains LPS, which is recognized by TLR4 located on the surface of phagocyte. The phagocytic activity can be assessed in both suspension and adhesive (on plastic or extracellular matrix) fractions of blood cells, as adhesion is not a requirement for phagocytosis by neutrophils [13].

A number of studies have shown a decrease in the phagocytic activity in people with age [14]. A decline in the phagocytic activity is considered in conjunction with other changes, e.g., decreased number of naïve T and B cells, increased systemic production of anti-inflammatory cytokines, reduced antigen presentation, and decreased secretion of specific antibodies.

Moreover, the age-related increase in the number of myeloid cells is accompanied by a decrease in the number of phagocytic cells in this population, as well as a decrease in the number of lymphoid cells. These phenomena are regarded as indications of the immune system aging [15]. Age-related activation of myelopoiesis may be an adaptive mechanism compensating for the loss of phagocytic function. Therefore, to accurately assess age-associated changes in the immune system activity, it is necessary to develop quantitative methods for analyzing the dynamics of phagocytosis at the level of individual cells.

An important quantitative parameter of phagocytosis is the phagocytic number – the average number of bacteria internalized by one phagocyte during the experiment. However, being an integrated parameter, the phagocytic number does not take into account the spatial position of a bacterium relative to the phagocyte membrane, leading to the loss of information on the kinetics of internalization and overestimation of the indicators of phagocytosis. In addition, routine assessment of the phagocytic number requires high-throughput methods for counting bacteria adhered to the surface and phagocytized into the cells in order to make a more accurate assessment of the phagocytic activity that would take into account the kinetics of the process.

Although microscopy can be used to estimate the phagocytic number, it is time-consuming, which imposes limitations on the method performance and reproducibility, as well as the statistical significance of the results. Flow cytometry is a high-throughput procedure and one of the simplest and most accessible methods for assessing the phagocytic activity, but its use does not imply visualization of the obtained data, which makes it difficult to quantitatively analyze the spatial position of particles in a cell. Here, we present a method developed to estimate the phagocytic number with simultaneous quantitative assessment of *E. coli* cells adhered to the surface and internalized by phagocytes using flow cytometry.

The method developed involves sequential conjugation of fixed bacterial cells with fluorescein-5-isothiocyanate (FITC) and biotin. After incubation with human peripheral blood, remaining external (adherent) bacteria are detected by staining with Alexa Fluor (AF405) conjugated with streptavidin. Streptavidin does not penetrate into phagocytes and selectively interacts with biotin covalently bound to proteins on the surface of *E. coli* cells. Therefore, the ingested bacteria would be labeled with FITC only, while externally attached bacteria would be positive for both AF405 and FITC (double-positive, DP), which allows to determine the location of each *E. coli* bacterium. When analyzed by flow cytometry, each individual cell was assessed for the fluorescence signal intensity, which allowed to distinguish several cell subpopulations and to suggest the existence of phagocytes with different numbers of internalized bacteria already at the initial stage of study.

We combined the data from flow cytometry and cell sorting with confocal microscopy imaging for quantification of phagocytized bacteria, thus validating the use of flow cytometry in routine studies requiring no visualization.

In addition to the time-consuming analysis by a combination of cell sorting and visual quantification by confocal microscopy, the samples were tested using an Amnis Flowsight imaging flow cytometer to accelerate the assessment of the spatial location of bacteria

in the cells. The double-staining procedure developed in this study significantly improved the accuracy of analysis of phagocytosis of bacterial cells using modern imaging flow cytometers.

MATERIALS AND METHODS

Conjugation of bacteria with FITC and biotin. Sterile glycerol (final concentration, 10%) was added to 20 ml of *E. coli* overnight culture (strain *DH5a*) grown from a single colony in LB medium and the resulting suspension was frozen at –20°C in 50-µl aliquots. One day before the experiment, 50 µl of the *E. coli* stock suspension in 10% glycerol was transferred to 10 ml of LB medium and grown overnight. The optical density of the cell suspension was determined with a Multiskan SkyHigh Microplate Spectrophotometer (Thermo Fisher, USA) at 540 nm. *E. coli* cells were diluted with LB medium to an optical density of 0.6, which corresponded to a concentration of 1.29×10^{10} bacteria per ml (according to a previously developed calibration curve). Next, 500 µl of *E. coli* cell suspension was centrifuged for 1 min at 2350*g*. The pellet was resuspended in 250 µl of phosphate buffered saline (PBS), 250 µl of fixative (10% neutral buffer formalin, Element Company, Russia) was added, and the bacterial suspension was thoroughly mixed by pipetting and vortexing. *E. coli* cells were fixed for 30 min at room temperature on a rotary mixer (10 rpm), washed 3 times with 500 µl of PBS, and pelleted by centrifugation for 2 min at 2350*g*. After the last centrifugation, the pellet was resuspended in 250 µl of PBS with 250 µl of borate buffer (50 mM, pH 9.0) and labeled with FITC (Lumiprobe, Russia) according to the manufacturer's instructions. For this purpose, dry FITC was dissolved at a concentration of 20 mg/ml in dimethyl sulfoxide, aliquoted into 10 µl, and stored at –80°C until use. Prepared FITC stock solution (1 µl) was added to 500 µl of bacterial suspension, and immediately mixed vigorously. The cell suspension was incubated for 16 h in the dark at 37°C with constant shaking in a Biosan TS-100 thermoshaker (400 rpm). After incubation, bacterial cells were washed three times with 500 µl of PBS and pelleted by centrifugation for 2 min at 2350*g*. After the last centrifugation, the pellet was resuspended in 200 µl of PBS; the cells were counted and stored at 4°C for a maximum of 24 h before use. Alternatively, the cells were resuspended in 200 µl of 10% glycerol solution, stored in aliquots at –20°C, and used for conjugation with FITC only. The efficiency of conjugation was assessed with a BD LSRFortessa flow cytometer from the fluorescence signal intensity in the FITC channel (488-nm laser; filter, 530/20 nm) in comparison with the control unconjugated fixed bacteria (Fig. 1). Next, FITC-labeled bacterial cells were conjugated with biotin using a FluoReporter Mini-biotin-XX Protein Labeling Kit (Thermo Fisher; cat. no. F6347) according to the manufacturer's instructions. Briefly, 200 µl of bacterial suspension was mixed with 20 µl of freshly prepared 1 M solution of sodium bicarbonate in water (pH 8.3-8.5) and 20 µl of active biotin ester (Component A) solution in deionized water was added (200 µl of water was added to a tube with dry Component A immediately before use, since the reactive form of biotin is quickly hydrolyzed in water). Bacterial cells were incubated with biotin for 2 h in the dark at room temperature at constant stirring in a Biosan TS-100 thermoshaker (400 rpm), washed twice with PBS by centrifugation for 2 min at 2350*g*, and resuspended in 200 µl of PBS. Sterile glycerol was added to a final concentration of 10%. After the concentration of labeled bacteria was determined using a cell-counting chamber and adjusted with PBS to 10^{10} cell/ml, the cells aliquoted in 20 µl, frozen, and stored at –20°C. All procedures were carried out under sterile conditions.

To test the efficiency of biotinylation procedure, 1 µl of streptavidin conjugated with AF405 (Invitrogen, USA, cat. no. S32351) was added to an aliquot of *E. coli* cells (300 µl, 1×10^7 *E. coli*/ml) and the mixture was incubated on ice for 30 min. The cells were washed with 1.2 ml of PBS, centrifuged for 2 min at 2350*g*, resuspended in 200 µl of PBS, and analyzed on a BD LSRFortessa flow cytometer to assess the DP cell population in the FITC and AF405 channels (405-nm laser, 450/50 nm filter) (Fig. 1).

All solutions were prepared in deionized water (18.2 MΩ·cm) produced by a Millipore Milli-Q IQ 7000 water purification system (Merck, USA).

Phagocytic test. Venous blood was collected from healthy volunteers using a system for vacuum blood collection into the tubes containing heparin sodium (Khimmedsnab, Russia) at the Sirius University Medical Center by a qualified personnel.

The concentration of leukocytes in the sample was determined using a Celltac MEK-7300K hematology analyzer (Nihon Kohden, Japan). This information was further used to calculate the amount of added bacteria based on the leukocyte : bacteria ratio of 1 : 20, in accordance with previously published works [16]. For the test, 100 µl of whole blood was pipetted into a polypropylene non-adhesive tube (Eppendorf, Germany, cat. no. 0030125150) and its temperature was stabilized in a CO_2 incubator (37°C, 5% CO_2) for 5 min. The phagocytic test was carried out in the suspension fraction of whole blood cells without using special procedures for cell adhesion to the surface [13]. Bacterial suspension was added to 100 µl of blood at a ratio of 20 bacterial cells per leukocyte and incubated for 1 h at 37°C in the CO_2 incubator. To stop phagocytosis, the samples were placed on ice (Fig. S1 in the Online Resource 1), [17].

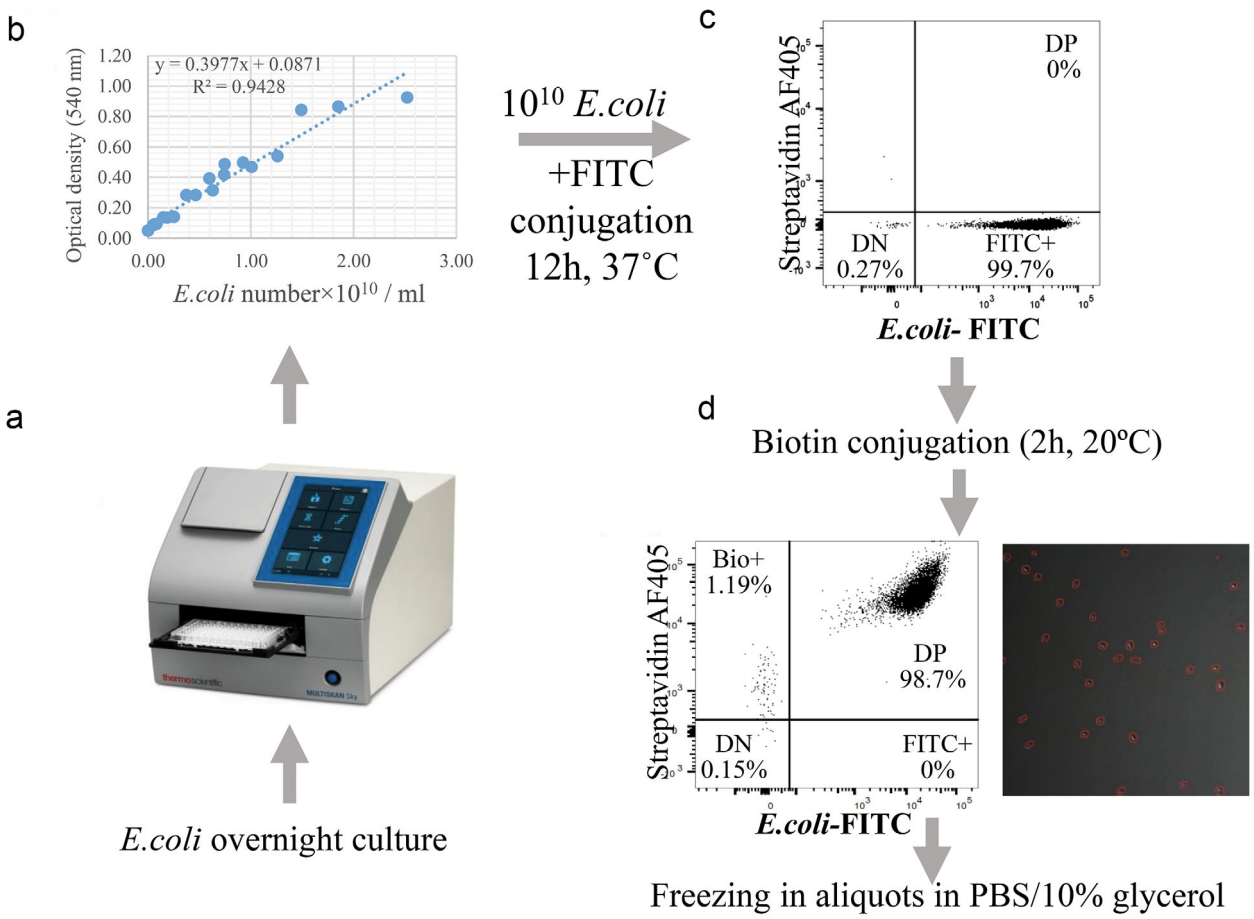

Fig. 1. Scheme of *E. coli* cell labeling (conjugation and quality control). Fixed bacterial cells were sequentially conjugated with FITC and biotin to be used for determining their spatial location inside and outside of phagocytes. The concentration of bacteria was determined by measuring the optical density (a) using a pre-calculated calibration curve (b). After conjugation with FITC, the uniformity of conjugation was verified by flow cytometry; 99.7% cells contained the FITC label (c). After subsequent conjugation with biotin, the uniformity of labeling was verified in both streptavidin-AF405 and FITC channels; the uniformity of conjugation was 98.7% for both labels (d). Before freezing the stock, the concentration of labeled bacteria was determined by the differential interference contrast (DIC) and fluorescence methods using a Countess 3 automated cell counter (Thermo Fisher).

Flow cytometry and cell sorting. Anti-CD45 antibody APC-eFluor780 (clone HI30, eBioscience, USA, cat. no. 47-0459-42; 1 : 100) was added to an aliquot of blood on ice after phagocytosis to label leukocytes; AF405-conjugated streptavidin (Invitrogen, cat. no. S32351; 1 : 100) was added to detect bacteria on the cell surface. The samples were incubated for 30 min in the dark on ice, washed with 1.4 ml of PBS, and centrifuged for 5 min at 330*g*. The supernatant was discarded and the pellet was resuspended by gentle pipetting in 100 µl of PBS; next, 900 µl of 1× BD FACS Lysing Solution (BD, cat. no. 349202) was added and the samples were incubated for 10 min in the dark at room temperature and then centrifuged for 5 min at 330*g*. The pellet was resuspended in 200 µl of PBS and stored at 4°C until analysis (see Fig. S1 in the Online Resource 1).

The compensation setup was carried out in an automated mode for a flow cytometer or a cell sorter using single-stained controls prepared as described above except the control for AF405, which was prepared by staining an aliquot of blood with biotin-conjugated anti-CD33 antibodies (clone AC104.3E3, Miltenyi; cat. no. 130-113-347) for 30 min on ice, followed by treatment with AF405-conjugated streptavidin and further processing as described above.

Preliminary analysis of the samples was carried out on a BD LSRFortessa flow cytometer. To determine the number of *E. coli* cells and their spatial location in white blood cells after phagocytosis, the cells were sorted with a Sony SH800 sorter equipped with 4 lasers (405, 488, 561, and 638 nm) and 100-micron nozzle chips and analyzed with a confocal microscope. The gaiting strategy implied sequential identification of single cells for the forward scatter (FSC) and then for the side scatter (SSC) according to the Area and Height pulse parameters, removal of cell debris based on the lighting scattering parameters, isolation of $CD45^+$ population, and identification of subpopulations of phagocytic leukocytes based on the fluorescence

signal intensity in the FITC and AF405 channels (Fig. S2 in the Online Resource 1). The cells were sorted into 5-ml polystyrene tubes with 1 ml of PBS (at least 10,000 cells for each leukocyte subpopulation).

Next, we used high-performance flow cytometry with visualization to determine the spatial location and number of bacteria inside and outside leukocytes. The work was performed using an Amnis FlowSight imaging flow cytometer (Cytek, USA) equipped with three lasers (405, 488, and 642 nm) that was provided by the Cytometry and Biomarkers Core Facility at the St. Petersburg Pasteur Research Institute of Epidemiology and Microbiology.

Confocal microscopy. After sorting, the cells were concentrated by centrifugation for 5 min at 330*g*, resuspended in 10 µl PBS and placed on charged glass slides (Polysine Adhesion Slides, Thermo Fisher). The slides were incubated in a humid chamber at room temperature for 30 min, covered with coverslips, and analyzed under an inverted laser scanning confocal ZEISS LSM 980 Airyscan microscope equipped with a 20× lens (Plan-Apochromat 20×, numerical aperture 0.8). The images in 4 channels were obtained by sequential scanning of two tracks: APC-eFluor 780 channel in the first track and AF405, FITC, and DIC (differential interference contrast) channels in the second track. APC-eFluor 780 was excited with a 639-nm laser [maximum power, 20 mV; acousto-optic tunable filter (AOTF) throughput, 2.6%] with signal detection at 647 to 757 nm (detector type, GaAsP; amplification, 713 V). AF405 was excited with a 405-nm laser (maximum power, 20 mV; AOTF throughput, 0.2%) with signal detection at 410 to 484 nm (detector type, GaAsP; amplification, 650 V). FITC was excited with a 488-nm laser (maximum power, 13 mV; AOTF throughput, 0.04%) with signal detection at 519 to 628 nm (detector type, Multialkali-PMT; amplification, 845 V). DIC images in transmitted light were obtained using the second track lasers (405 and 488 nm) with a T-PMT detection at 300 to 900 nm (Multialkali-PMT detector; amplification, 368 V). The following scanning parameters were used: scanning zoom, 8×; image size, 429×429 pixel; pixel time (signal accumulation time), 4.91 microsecond; pixel size, dx = dy = 0.124 µm. The images were obtained using the ZEN Blue 3.2 (Zeiss) software.

Software. The results were processed in Microsoft Excel 2019. Flow cytometry data were analyzed with BD FlowJo v. 10.9.0; Amnis FlowSight data were analyzed with Amnis IDEAS 6.2; confocal microscopy data were analyzed with ImageJ/Fiji v. 1.54f [18].

RESULTS AND DISCUSSION

Quantitative analysis of phagocytosis by cell sorting and microscopy. After phagocytosis, several subpopulations of CD45$^+$ leukocytes were gated by the granularity, size and *E. coli* fluorescence (Fig. 2). To analyze the distribution of internalized or surface-adhered bacteria in granulocytes, monocytes, and lymphocytes, these cell populations were sorted with a Sony SH800 sorter (see Fig. 2 and Fig. S2 in the Online Resource 1 for the gating strategy) and analyzed under a ZEISS LSM 980 Airyscan confocal microscope. After establishing the protocol for the procedure, cell sorting was carried out three times using blood samples of three donors.

Comparison of cell sorting and microscopy data is presented in Fig. 3. The most abundant population was a double-negative (DN) subpopulation (71.2% of all CD45$^+$ cells). None of these cells contained *E. coli* bacteria inside or on the surface, as was found by the analysis of 74 confocal microscopy images of the sorted DN cells from three donors. DIM cells (cells whose fluorescence intensity was 10 times brighter than the fluorescence of DN cells) demonstrated dull fluorescence in the FITC channel. Out of 33 DIM cells analyzed under a microscope, only one contained bacteria; all other cells had a slightly fluorescent cytoplasm that was likely a background autofluorescence resulting from the uptake of the debris of FITC-conjugated bacteria. The MID subpopulation forms a distinct cluster with FITC fluorescence approximately 10 times brighter than the fluorescence of DIM cells. The fluorescence intensity of MID cells in the AF405 channel corresponded to the autofluorescence of DN cells. This indicates that the MID population consisted of cells that have phagocytized bacteria and did not contain *E. coli* on the surface.

Analysis of confocal microscopy images (total of 151 cells) confirmed this assumption. The phagocytic number in the MID population varied from 1 to 5 (average value, 1.87 bacteria per cell). DP cells (3% of all cells) contained bacteria either on the surface only or on the surface and inside the cells (Fig. 3). The average number of bacteria inside the cells in the DP population (based on analysis of 51 cells) was 0.67 bacteria per cell (value range, 0-16); the average number of bacteria outside the cells was 1.41 (value range, 1-6). Hence, the DP population was extremely heterogeneous and can be further divided into several subpopulations.

Visualization of phagocytes in the flow using double staining revealed the presence of a significant amount of *E. coli* on the surface of the cells. Although sequential use of cell sorting and confocal microscopy allows to assess the quantity and spatial location of bacteria in phagocytes, such analysis is laborious and time-consuming. The use of flow cytometry only makes it possible to estimate the number of *E. coli* bacteria inside the phagocytes based on fluorescence, but does not allow to quantify phagocytosis when the bacteria are located simultaneously inside the cells and on their surface.

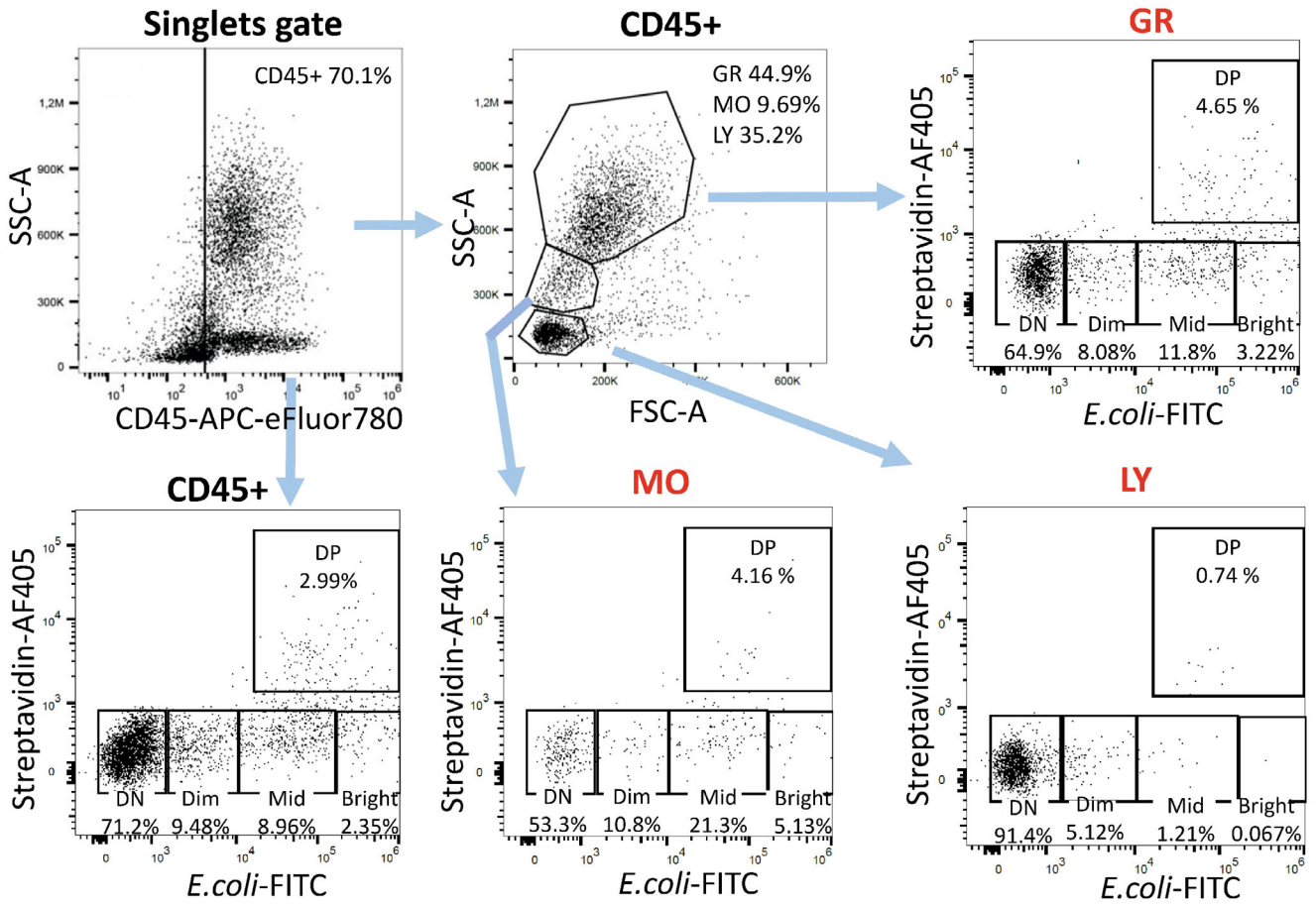

Fig. 2. Cell analysis and gating strategy for a Sony SH800 sorter: leukocytes (CD45⁺) were collected from the singlets gate and then sorted based on the fluorescence intensity and location of bacteria (*E. coli*) on double negative (DN) non-phagocytizing cells; DIM, cells whose fluorescence was an order of magnitude brighter vs. DN cells; MID, cells with moderate fluorescence (more than an order of magnitude compared to DIM cells); Bright, cells with the highest fluorescence intensity; DP, double-positive (FITC- and AF405-labeled) bacteria on the surface of phagocytes (lower left panel). For identification of cell subpopulations, the cells were gated based on the granularity (SSC) and size (FSC): GR, granulocytes; MO, monocytes; LY, lymphocytes (see Fig. S2 in the Online Resource 1 for more information on the gating strategy).

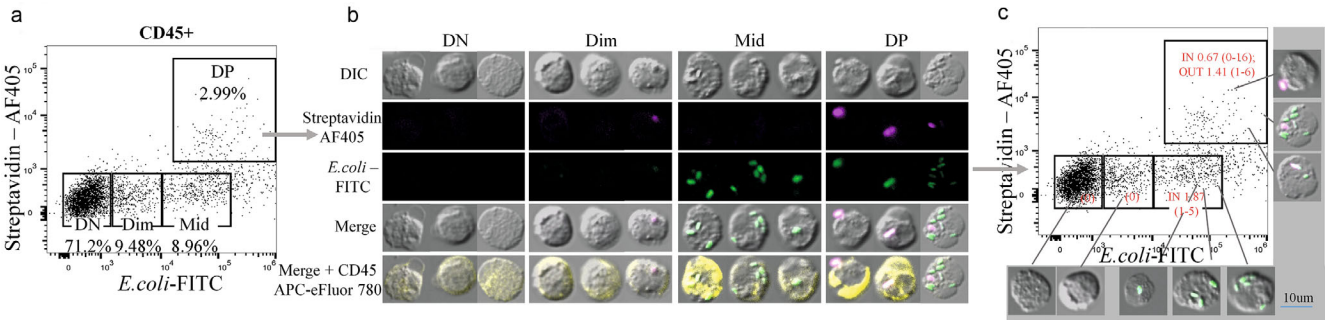

Fig. 3. Results of cell sorting of phagocytic leukocytes (CD45⁺) (a) and analysis of sorted populations by confocal microscopy (b). DN cells contained no bacteria; DIM cells demonstrated autofluorescence but contained no bacteria; MID cells contained 1-5 bacteria per cell inside the cells; DP cell contained bacterial cells both inside the cells or on the cell surface only. Overlapped DIC and fluorescence (FITC, AF405) images are designated as “merge”. c) Individual cell images as examples of leukocytes with different number of *E. coli*. Red figures indicate the average number of *E. coli* cells inside (IN) and outside (OUT) of leukocytes; the value range is shown in parentheses. The number of independent experiments, n = 3.

We used an Amnis FlowSight imaging flow cytometer to improve the quantitative analysis of phagocytosis in cell populations containing bacteria both inside and on the cell surface and to obtain more statistically reliable values of phagocytic count. This instrument also allows to photograph the cells in a flow at a rate

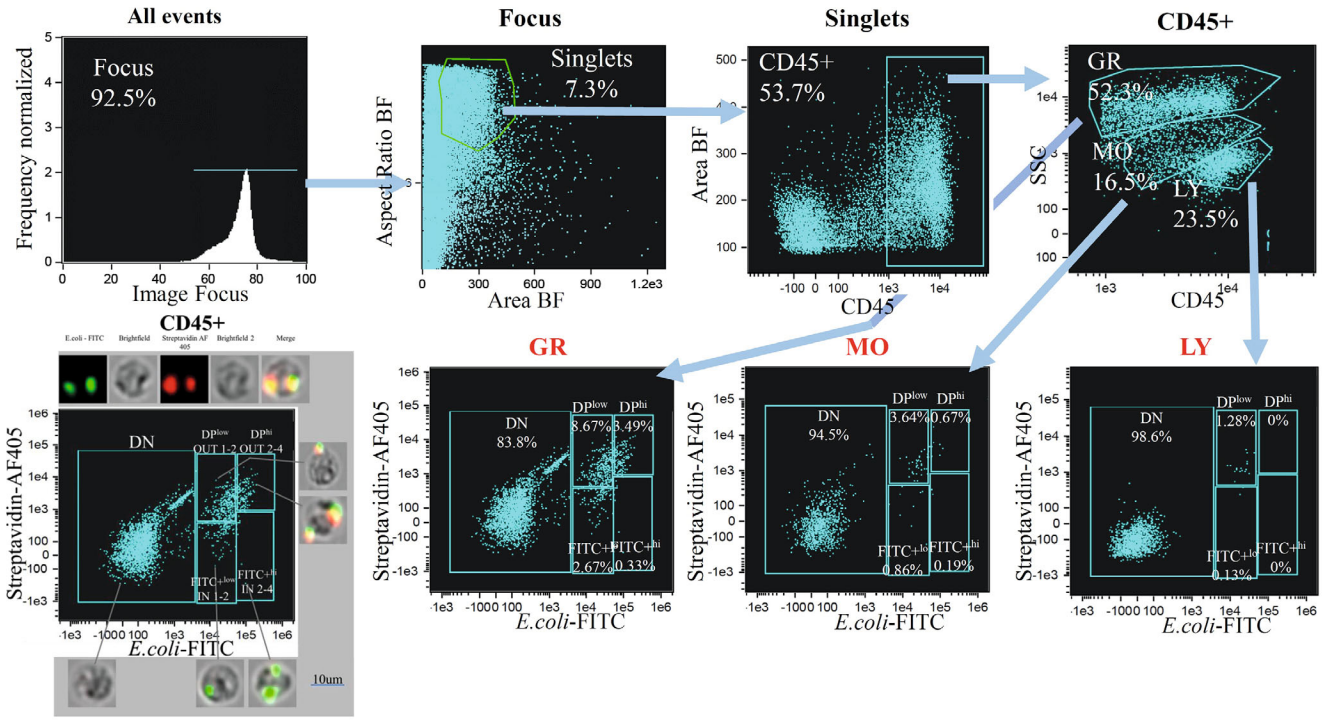

Fig. 4. Gating strategy for cell analysis on an Amnis Flowsight imaging flow cytometer and examples of visualization of individual cells from the CD45⁺ population. The numbers indicate the percentage of cells in the population and the number of bacteria inside (IN) and outside (OUT) the cells. The number of analyzed cells in individual populations was up to 352 (Fig. S3 in the Online Resource 1). The number of independent experiments, n = 3.

of up to several thousand per second and to analyze the spatial position of microbial particles in the phagocytes. We evaluated the effectiveness of this approach by analyzing blood samples after phagocytosis. Figure 4 shows the gating strategy for experiments on an Amnis FlowSight imaging flow cytometer and summarized visualization data with images obtained by a cytometer (bottom row, left graph and images around it). The photographs above the graph represents the images for different fluorescence channels (FITC, all bacteria; Streptavidin-AF405, bacteria on the phagocytic leukocyte surface), bright-field microscopy images (Brightfield and Brightfield 2), and channel overlay (Merge). Analysis of cell images allows to conclude that non-internalized bacteria were double stained and located on the surface of phagocytes, while engulfed bacteria were detected only in the FITC channel. Based on the fluorescence signal intensity, four cell subpopulations could be distinguished that differed in the number of *E. coli* located inside the cells and on the cell surface. DP^{low} cells (fluorescence intensity in the FITC channel, 10^4-10^5) contained 1-2 bacteria on the surface; DP^{hi} cells subpopulation (the brightest subpopulation of DP cells; fluorescence intensity in FITC channel, above 10^5) contained 2-4 bacteria on the surface; phagocytes of the $FITC^{low}$ subpopulation contained 1-2 bacteria inside the cell, and phagocytes of the $FITC^{hi}$ subpopulation had 2-4 bacteria inside the cell.

We also tested the effectiveness of the built-in IDEAS 6.2 software which recognizes the location of bacteria inside or outside the cell based on the images taken by the cytometer. The results of the detection of bacteria on the cell surface (but not inside the cell) provided by the program and obtained by the analysis of double-staining data coincide by 94.9% (Fig. 5a, *E. coli* detected outside the gate), indicating that the program was indeed able to recognize FITC- and AF405-positive bacterial cells on the phagocyte surface. Since the program makes an assessment based on the cell parameters extracted from an image in a single projection, in 70% of the cases, these bacteria were recognized by the program as being inside cells, although according to the double staining, they were on the cell surface (Fig. 5b, *E. coli* detected inside the gate), which is due to the technical limitations of the imaging capabilities of an imaging flow cytometer. Figure 5c (lymphocytes, LY gate) shows the results of phagocytosis by lymphocytes: 98.6% of these cells were double-negative for FITC and streptavidin-AF405 (i.e., did not phagocytize). However, some cells (1.28%) were double-positive, indicating that lymphocytes are capable of retaining *E. coli* on the surface without internalization (at least, within an hour of incubation with whole blood).

There are currently many objects used to analyze phagocytosis, for example, *E. coli* cells labeled with pH-dependent dyes. However, the use of these reagents

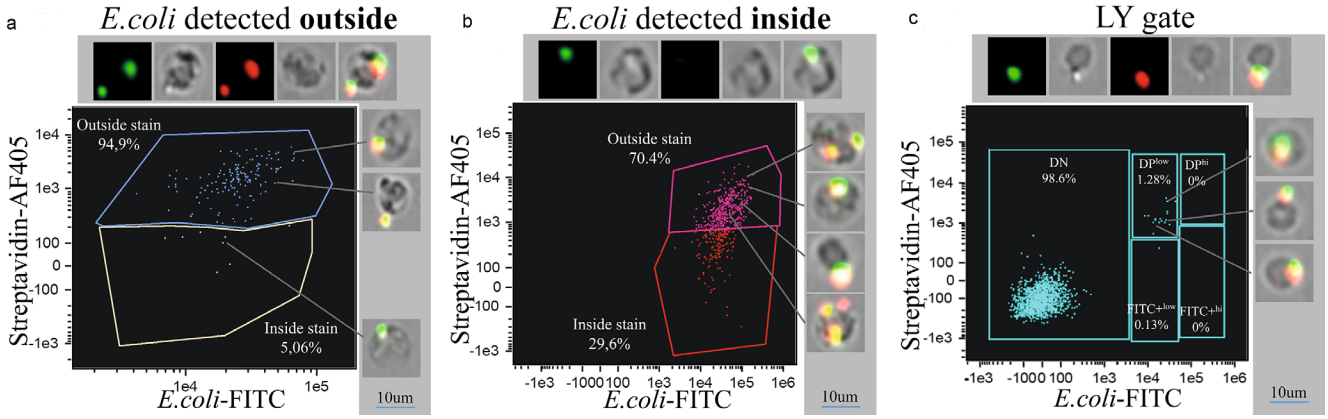

Fig. 5. a) *E. coli* cells that were detected by the program as being located on the phagocytes; 94.9% of these cells were indeed positive for both FITC and AF405, i.e., adhered to the phagocyte surface. b) Bacteria that were detected by the program as being inside the cells. However, 70.4% of these cells were positive for both FITC and AF405; c) Lymphocyte (LY) gate. Although the program detected some cells (1.28%) in the lymphocyte population as phagocytic, all these cells contained *E. coli* bacteria on the surface (according to double staining). The top panels show the channels (from left to right): FITC (*E. coli*), Brightfield 1, AF405 (biotin-streptavidin, *E. coli*), Brightfield 2, and an overlay of all channels. Right and central panels show cells as dots in flow cytometry plots (see Fig. S3 in the Online Resource 1 for more cell images).

requires the replacement of blood plasma with a special buffer to control pH, which negatively affects cell viability and leads to distorted results [19]. Moreover, when studying phagocytosis in whole blood *in vivo*, it is difficult to control the plasma pH, and therefore the use of bacteria labeled with pH-dependent dyes is limited and does not allow distinguish between internalized *E. coli* cells and cells on the phagocyte surface. Single-color labeling without the ability to distinguish between the bacteria located inside and outside the cells leads to inaccurate results [19, 20]. At the same time, the application of antibodies specific to antigens of individual bacterial species [21] is not universal and requires the development of new species-specific antibodies when studying phagocytosis efficiency for different bacterial species. The use of FITC- and biotin-labeled bacteria of any species provides easy identification of nonphagocytized bacteria by surface staining with AF405-conjugated streptavidin and facilitates their detection by confocal microscopy. However, despite a high accuracy, confocal microscopy is not a high-throughput method. The development of novel flow cytometry imaging techniques makes it possible to process large sets of data. Here, we used imaging flow cytometry and developed a phagocytized agent allowing to perform analysis with a high throughput and accuracy. Therefore, double labeling helps to distinguish between intracellular and surface location of bacteria at any stage of phagocytosis in whole blood and to assess the kinetics of this process.

Thus, analysis of images obtained with the Amnis FlowSight cytometer software showed that the provided program identified bacteria inside and on the surface of cells with a low accuracy. For example, some lymphocytes were detected by the program as phagocytic, but not by the double-staining (Fig. 5c). Therefore, the recognition algorithms of in the imaging flow cytometer software might overestimate the phagocytosis activity when using traditional objects for phagocytosis, while the method developed by us (*E. coli* conjugation with double label followed by the phagocytic test) can significantly increase the accuracy of the results and can be used to assess quantitative and temporal dynamics of pathogen uptake.

Although the proposed method has some limitations, they can be easily overcome. It is known that some types of bacteria contain avidins (proteins with a high affinity for biotin) in their cell wall [22]. In this case, direct detection using fluorochrome-conjugated biotin is recommended instead of conjugation of bacteria with biotin. If the content of avidins in the bacterial cell wall is too low for detection, it might be efficient to use an excess of reactive biotin ester for the conjugation of bacteria and subsequent staining with streptavidin. As an alternative, avidin epitopes can be blocked with biotin and then cell is labeled with a reactive biotin ester at protein amino groups.

CONCLUSION

This study presents the results of quantitative analysis of phagocytosis using sorting and subsequent visualization of the analyzed populations. Using cell sorting techniques and confocal microscopy, fluorescence values were compared with data on the number and location of *E. coli* relative to phagocytic blood cell populations. It was found that within one hour of phagocytosis, the majority of granulocytes and monocytes completed the process of *E. coli* internalization.

However, when an excess of *E. coli* cells was added, 20% of phagocytes adhered bacteria on the cell surface without their internalization. We hypothesize that along with phagocytosis, retention of bacteria on the lymphocyte surface may be an important component of antimicrobial function of the immunity system.

Quantitative analysis of phagocytic number in minor cell populations that contain bacteria both intracellularly and on the cell surface usually requires the use of time-consuming confocal microscopy followed by data analysis and 3D reconstruction in order to determine the location of these bacteria. The use of imaging flow cytometry in combination with dual-labeled *E. coli* preparations allows high-throughput and high-accuracy quantification of bacteria inside and outside the cells. Double-staining of *E. coli* has significantly improved the accuracy of flow cytometry data with cell visualization in the flow.

It was also shown that the majority of FITC positive lymphocytes retained bacteria externally, without internalization, and only a minor fraction of these cells was capable of phagocytosis. Further analysis of subpopulations that rapidly phagocytize bacteria or retain them on the surface by imaging flow cytometry will provide more precise understanding of the function of individual cell populations in the processes of adaptive and innate immunity.

Supplementary information. The online version contains supplementary material available at https://doi.org/10.1134/S0006297924050122.

Acknowledgments. The authors thank S. A. Nedospasov, O. K. Batsunov, and V. V. Zarubaev, for assistance with the study; Resource Center for Cellular Technology and Immunology at Sirius University for Science and Technology for providing equipment for the experiments; Core Facility “Cytometry and Biomarkers” at the Pasteur Research Institute of Epidemiology and Microbiology in St. Petersburg for providing an Amnis FlowSight imaging flow cytometer (Cytek, USA).

Contributions. E.V.L., A.N.S., S.A.C., V.S.L., and N.A.A. conducted the experiments; E.V.L., N.A.A., A.N.S., and S.A.R. discussed the results; E.V.L., N.A.A., A.N.S., M.Yu.B., and V.S.L. calculated and analyzed results; E.V.L. and S.A.R. wrote the text of the article; E.V.L., A.N.S., S.A.C., V.S.L., N.A.A., M.Yu.B., and S.A.R. edited the manuscript; S.A.R. developed the research concept and supervised the study.

Funding. This study was supported by the Russian Science Foundation (project no. 23-15-00443; https://rscf.ru/project/23-15-00443/ [in Russian]; analysis of phagocytosis by flow cytometry and confocal microscopy, analysis of the results, preparation of the manuscript) and the Ministry of Science and Higher Education of the Russian Federation (agreement no. 075-10-2021-093; project NIR-IMB-2102; preparation of double-labeled bacteria, quantitative analysis, and validation of the bacterial preparation on an Amnis FlowSight cytometer).

Ethics declarations. All procedures performed in the study involving human subjects complied with the national ethical standards, the 1964 Declaration of Helsinki and its subsequent amendments and were approved by the Bioethics Committee of Sirius University (protocol from 03/06/2023). Informed voluntary consent was obtained from all participants prior to the collection of blood sample. The authors of this work declare that they have no conflicts of interest.

REFERENCES

1. Lancaster, C. E., Ho, C. Y., Hipolito, V. E., Botelho, R. J., and Terebiznik, M. R. (2019) Phagocytosis: what’s on the menu? *Biochem. Cell Biol.*, **97**, 21-29, doi: 10.1139/bcb-2018-0008.
2. Carneiro, V. M. A., Bezerra, A. C. B., Guimarães, M. D. C. M., and Muniz-Junqueira, M. I. (2012) Decreased phagocytic function in neutrophils and monocytes from peripheral blood in periodontal disease, *J. Appl. Oral Sci.*, **20**, 503-509, doi: 10.1590/s1678-77572012000500002.
3. Singh, R., Belchamber, K. B. R., Fenwick, P. S., Chana, K., Donaldson, G., Wedzicha, J. A., Barnes, P. J., Donnelly, L. E., and COPDMAP consortium (2021) Defective monocyte-derived macrophage phagocytosis is associated with exacerbation frequency in COPD, *Respirat. Res.*, **22**, 113, doi: 10.1186/s12931-021-01718-8.
4. Nakahashi-Oda, C., Fujiyama, S., Nakazawa, Y., Kanemaru, K., Wang, Y., Lyu, W., Shichita, T., Kitaura, J., and Shibuya, A. (2021) CD300a blockade enhances efferocytosis by infiltrating myeloid cells and ameliorates neuronal deficit after ischemic stroke, *Sci. Immunol.*, **6**, eabe7915, doi: 10.1126/sciimmunol.abe7915.
5. Kelley, S. M., and Ravichandran, K. S. (2021) Putting the brakes on phagocytosis: “don’t-eat-me” signaling in physiology and disease, *EMBO Rep.*, **22**, e52564, doi: 10.15252/embr.202152564.
6. Tang, Z., Davidson, D., Li, R., Zhong, M. C., Qian, J., Chen, J., and Veillette, A. (2021) Inflammatory macrophages exploit unconventional pro-phagocytic integrins for phagocytosis and anti-tumor immunity, *Cell Rep.*, **37**, 110111, doi: 10.1016/j.celrep.2021.110111.
7. Uribe-Querol, E., and Rosales, C. (2017) Control of phagocytosis by microbial pathogens, *Front. Immunol.*, **8**, 1368, doi: 10.3389/fimmu.2017.01368.
8. Gagnon, E., Duclos, S., Rondeau, C., Chevet, E., Cameron, P. H., Steele-Mortimer, O., Paiement, J., Bergeron, J. J. M., and Desjardins, M. (2002) Endoplasmic reticulum-mediated phagocytosis is a mechanism of entry into macrophages, *Cell*, **110**, 119-131, doi: 10.1016/s0092-8674(02)00797-3.

9. Dempsey, L. A. (2019) Inhibiting phagocytosis, *Nat. Immunol.*, **20.9**, 1089, doi: 10.1038/s41590-019-0485-z.
10. Cruz, F. M., Chan, A., and Rock, K. L. (2023) Pathways of MHC I cross-presentation of exogenous antigens, *Semin. Immunol.*, **66**, 101729, doi: 10.1016/j.smim.2023.101729.
11. Porpodis, K., Domvri, K., Zarogoulidis, P., Petridis, D., Tsirgogianni, K., Papaioannou, A., Hatzizisi, O., Kioumis, I., Liaka, A., Kikidaki, V., Lampaki, S., Organtzis, J., and Zarogoulidis, K. (2015) Roflumilast, a phosphodiesterase-4 inhibitor, induces phagocytic activity in Greek COPD patients, *Int. J. Chron. Obstruct. Pulmon. Dis.*, **10**, 1123-1128, doi: 10.2147/COPD.S83205.
12. Morais, T. C., Honorio-França, A. C., Fujimori, M., de Quental, O. B., Pessoa, R. S., França, E. L., and de Abreu, L. C. (2019) Melatonin action on the activity of phagocytes from the colostrum of obese women, *Medicina*, **55**, 625, doi: 10.3390/medicina55100625.
13. Garcia-Seyda, N., Seveau, V., Manca, F., Biarnes-Pelicot, M., Valignat, M. P., Bajenoff, M., and Theodoly, O. (2021) Human neutrophils swim and phagocytise bacteria, *Biol. Cell*, **113**, 28-38, doi: 10.1111/boc.202000084.
14. Li, W. (2013) Phagocyte dysfunction, tissue aging and degeneration, *Ageing Res. Rev.*, **12**, 1005-1012, doi: 10.1016/j.arr.2013.05.006.
15. Ciabattini, A., Nardini, C., Santoro, F., Garagnani, P., Franceschi, C., and Medaglini, D. (2018) Vaccination in the elderly: the challenge of immune changes with aging, *Semin. Immunol.*, **40**, 83-94, doi: 10.1016/j.smim.2018.10.010.
16. Robinson, J. P., Carter, W. O., and Narayanan, P. (1997) Functional assays by flow cytometry, in *Manual of Clinical Laboratory Immunology. Volume Immune Cell Phenotyping and Flow Cytometric Analysis: Am. Soc. Microbiol.* (Rose, Ed., Folds, J. D., Lane, H. C., and Nakumura, R., eds) 5, pp. 245-254.
17. Serrander, L., Skarman, P., Rasmussen, B., Witke, W., Lew, D. P., Krause, K. H., Stendahl, O., and Nüße, O. (2000) Selective inhibition of IgG-mediated phagocytosis in gelsolin-deficient murine neutrophils, *J. Immunol.*, **165**, 2451-2457, doi: 10.4049/jimmunol.165.5.2451.
18. Lindner, B., Burkard, T., and Schuler, M. (2020) Phagocytosis assays with different pH-sensitive fluorescent particles and various readouts, *Biotechniques*, **68**, 245-250, doi: 10.2144/btn-2020-0003.
19. Yang, F., Zhang, F., Yang, L., Li, H., and Zhou, Y. (2021) Establishment of the reference intervals of whole blood neutrophil phagocytosis by flow cytometry, *J. Clin. Lab. Analysis*, **35**, e23884, doi: 10.1002/jcla.23884.
20. Jackaman, C., Tomay, F., Duong, L., Razak, N. B. A., Pixley, F. J., Metharom, P., and Nelson, D. J. (2017) Aging and cancer: the role of macrophages and neutrophils, *Ageing Res. Rev.*, **36**, 105-116, doi: 10.1016/j.arr.2017.03.008.
21. DeLoid, G. M., Sulahian, T. H., Imrich, A., and Kobzik, L. (2009) Heterogeneity in macrophage phagocytosis of *Staphylococcus aureus* strains: high-throughput scanning cytometry-based analysis, *PLoS One*, **4**, e6209, doi: 10.1371/journal.pone.0006209.
22. Laitinen, O. H., Kuusela, T. P., Kukkurainen, S., Nurminen, A., Sinkkonen, A., and Hytönen, V. P. (2021) Bacterial avidins are a widely distributed protein family in Actinobacteria, Proteobacteria and Bacteroidetes, *BMC Ecol. Evol.*, **21**, 1-53, doi: 10.1186/s12862-021-01784-y.